

Water Resources Research

RESEARCH ARTICLE

10.1029/2020WR028777

Key Points:

- $\delta^{18}\text{O}$ and $\delta^2\text{H}$ have summer values in tap water distinct from local precipitation in the Denver area
- Most urban baseflow in 13 urban streams in the Denver area was sourced from tap water based on water stable isotopes
- Tap water contributions to the streams were mostly from excess lawn irrigation as determined using infrastructure leakage reports

Supporting Information:

Supporting Information may be found in the online version of this article.

Correspondence to:

A. S. Bhaskar,
aditi.bhaskar@colostate.edu

Citation:

Fillo, N. K., Bhaskar, A. S., & Jefferson, A. J. (2021). Lawn irrigation contributions to semi-arid urban baseflow based on water-stable isotopes. *Water Resources Research*, 57, e2020WR028777. <https://doi.org/10.1029/2020WR028777>

Received 12 SEP 2020

Accepted 12 JUL 2021

© 2021. The Authors.

This is an open access article under the terms of the [Creative Commons Attribution-NonCommercial-NoDerivs License](#), which permits use and distribution in any medium, provided the original work is properly cited, the use is non-commercial and no modifications or adaptations are made.

Lawn Irrigation Contributions to Semi-Arid Urban Baseflow Based on Water-Stable Isotopes

Noelle K. Fillo^{1,2} , Aditi S. Bhaskar¹ , and Anne J. Jefferson³ 

¹Department of Civil and Environmental Engineering, Colorado State University, Fort Collins, CO, USA, ²Now at WEST Consultants, Inc., Tempe, AZ, USA, ³Department of Geology, Kent State University, Kent, OH, USA

Abstract In semi-arid cities, urbanization can lead to elevated baseflow during summer months. One potential source for additional water is lawn irrigation. We sought to quantify lawn irrigation contributions to summertime baseflow in Denver, Colorado, USA using water-stable isotope ($\delta^{18}\text{O}$ and $\delta^2\text{H}$) analysis of surface water, tap water, and precipitation. If lawn irrigation contributed significantly to baseflow, we predicted the isotopic composition of Denver's urban streams would more closely resemble local tap water than precipitation or streamflow from nearby grassland watersheds. We expected tap water to be distinctive due to local water providers importing source water from high elevations. Thirteen urban streams and two grassland streams were selected for sampling. None of the streams had high-elevation headwaters or wastewater effluent, and the grassland streams did not receive irrigation. Tap water was sampled from five water service areas. The grassland streams flowed for 60% of summer 2019 while urban streams flowed for 90%–100% of the summer. An isotope mixing analysis using tap and precipitation end-members over a two week antecedent period estimated that tap water contributed $65\% \pm 10\%$ – $93\% \pm 3\%$ with a mean of 80% of urban baseflow on specific days in late summer. After taking contributions from infrastructure leakage into account, we estimated that lawn irrigation return flows made up $32\% \pm 10\%$ – $82\% \pm 21\%$ of analyzed baseflow. Quantifying lawn irrigation contributions to urban baseflow provides a basis for understanding how changes to lawn irrigation efficiency would affect water yield in the Denver metropolitan area.

Plain Language Summary Excess lawn irrigation may contribute to flow in urban streams when more water is applied than plants can use or when sidewalks or driveways receive water from misaimed sprinklers. We have applied a new approach to estimating how much flow in streams originally came from excess lawn irrigation by using a tracer that is different between tap water in the Denver, Colorado USA area and local rain. We applied this approach to 13 urban streams and two grassland streams in the Denver area. We found that, on the dry weather days analyzed, over 65% of flow in urban streams was from tap water, and lawn irrigation was a larger source of water in the streams than leaking water pipes. This work gives a new way to analyze how much flow is coming from different sources in urban areas, which is important for understanding consequences for water quality and water rights for downstream users.

1. Introduction

Semi-arid and arid cities are growing rapidly, often in river basins where water is already overallocated (Sabo et al., 2010). Previous strategies to increase water supply through transbasin imports have become infeasible, so cities have turned to demand management strategies such as efficiency and conservation in municipal outdoor use (Gleick, 2010; Gonzales & Ajami, 2017; Quesnel & Ajami, 2017). Meanwhile, increased urban growth not only stresses water supply systems, but also directly and dramatically alters urban streamflow. While much attention has focused on urban peak flows, alterations to urban baseflow can have magnified ecological consequences in streams with little baseflow under natural conditions (Rolls et al., 2012; Strange et al., 1999).

Impervious surfaces alone do not explain changes in urban baseflow (Hopkins et al., 2015). Post-development baseflow has the potential to rise, fall, or remain consistent when compared to pre-development observations (Bhaskar, Beesley, et al., 2016). Potential urban causes of rising baseflow include wastewater effluent outfalls (Dennehy et al., 1993; Townsend-Small et al., 2013), channel deepening and riparian

vegetation removal (Hibbs et al., 2012), leaking water infrastructure (Garcia-Fresca & Sharp, 2005; Lerner, 2002), widespread stormwater infiltration along with reductions in vegetative cover (Barron et al., 2013; Bhaskar, Hogan, & Archfield, 2016), and lawn irrigation return flows (LIRFs) (Berg et al., 1996; Grimmond & Oke, 1986; Passarello et al., 2012; Sanzana et al., 2019).

Of particular interest to growing, water-stressed, semi-arid cities are ways to reduce urban irrigation, as urban irrigation generally makes up more than 50% of annual water use (Cooley et al., 2019; DeOreo et al., 2016; Gober et al., 2016). LIRF is water originally intended for plant growth (including lawns and other residential vegetation) that is instead transported to streams via alternative flow paths. Potential alternative flow paths include (a) surface runoff directly into a stream or into a storm sewer system that then drains to a local stream and (b) infiltration of irrigation to the saturated zone and subsequent discharge from the subsurface to a stream. The fraction of applied irrigation water that becomes LIRF depends strongly on the irrigation method (e.g., sprinkler vs. drip), timing, and amount (Bijoor et al., 2014; Oad & DiSpigno, 1997), but also can vary with vegetation type, climate conditions, and soil type. Previous work investigating the effects of lawn-watering restrictions found that streamflow in an urban watershed in Los Angeles, California was seven times larger compared to streamflow in a nearby nonurban watershed before the restrictions were implemented (Manago & Hogue, 2017). Urban streamflow dropped by 70% during the restriction period, while the nonurban watershed experienced no statistically significant changes in streamflow (Manago & Hogue, 2017). Lawn irrigation contributions to streamflow particularly are of interest as the next major focus of municipal water conservation in semi-arid and arid cities is reduction of urban irrigation (Gober et al., 2016).

Assessments of the contributions from different sources to streamflow can be performed by isotopic or geochemical tracers. Water balance approaches alone are often confounded by large uncertainties in multiple components (Kampf et al., 2020) and cannot separate streamflow contributors by source without other tracers. Stable isotopes in water have been used extensively in understanding hydrological and ecological processes (e.g., de Wet et al., 2020). In urban settings, they have been used to study public water supply systems and effects of urbanization and climate on stream water–groundwater connectivity (Ehleringer et al., 2016; Gabor et al., 2017; Hibbs et al., 2012; Jameel et al., 2018; Jefferson et al., 2015; Kuhlemann et al., 2020, 2021; Shah et al., 2019). Stable isotopes have been used to quantify the portion of urban streamflow from tap water, yielding low values in exurban Southern California and in San Diego streams during stormflow (Hibbs et al., 2012; Wallace et al., 2021) to 95% in Austin, Texas (Beal et al., 2020; Christian et al., 2011). The use of geochemical and isotopic tracers has been able to quantify the contributions of tap water to streamflow, but cannot distinguish between pipe leakage and lawn irrigation, as these are both sourced from tap water and therefore not geochemically or isotopically distinct.

The Denver, Colorado, USA metropolitan area is hypothesized to be an area where LIRF is an important contributor to stream baseflow. Denver receives an average annual precipitation of 391 mm with the highest precipitation between April and September (NOAA, 2020). In this semi-arid region, 62% of residential water is used outdoors and 74% of surveyed homes in Denver have “in-ground irrigation/sprinkling systems,” mostly with automatic timers (DeOreo et al., 2016). The impact of this widespread urban irrigation on stream baseflow in the Denver area has yet to be determined.

Our goal was to answer the questions: (a) how much summer baseflow in Denver area streams comes from tap water sources and (b) how much of the tap water contribution can be attributed to lawn irrigation as compared to infrastructure loss. In contrast to previous work investigating drought restrictions, we investigated a period of typical lawn irrigation. We answered the first question using water-stable isotopes as a tracer of tap water and the second question using reported infrastructure losses from tap water providers. Isotope values in surface water from urban and grassland watersheds were compared to tap water and precipitation to determine the relative contributions to Denver baseflow. If lawn irrigation contributes significantly to baseflow, we predicted the isotopic composition of Denver’s urban streams would more closely resemble the local tap water than streamflow from nearby grassland watersheds. We expected the tap water to be distinctive since local water providers do not source their tap water locally. Instead, much of the Denver metropolitan area’s tap water is imported from high-elevation collection areas.

2. Methods

2.1. Denver Metropolitan Study Areas

Thirteen urban watersheds and two grassland watersheds in the Denver metropolitan area were included in the study (Figure 1, Table 1). The watersheds were delineated based on the National Hydrography Dataset and a 10 m digital elevation model (USDA, 2018) in ArcGIS Pro (ESRI; Fillo, 2020). Urban stream samples were taken near USGS stream gages, which generally operate from April 1 to September 30. The grassland watersheds were located in the Rocky Flats National Wildlife Refuge, and their sampling locations were chosen based on proximity to walking trails and a United States Department of Energy (DOE) stream gage. None of the study watersheds had wastewater discharge (<https://erams.com/catena/>) and the grassland streams did not receive any irrigation. None of our watersheds contained known groundwater upwelling points or were connected to the South Platte alluvial aquifer (City and County of Denver, 2019), so we were not concerned with deep groundwater inputs to our streams.

The Denver metropolitan area was serviced by multiple tap water providers (Figure 1). Service area boundaries for these water providers were obtained from public GIS databases, requested from the water providers, or hand-digitized based on an image, and edited in some cases to account for recent service area changes (Fillo, 2020). In addition to water provider service area boundaries (Figure 1), we were also interested in the water provider collection areas and their associated elevations (Table 2). All the water providers serving our study watersheds used high elevation surface water sources in the Rocky Mountains west of Denver, and only in one case was this supplemented with deep groundwater (Centennial Water and Sanitation District; Table 2).

In comparison to the elevation of the water provider collection areas (Table 2), the elevations of our study watersheds were low. The mean elevations of our study watersheds ranged from 1,628–1,891 m above sea level (Table 1), and none had high-elevation headwaters. The maximum study watershed elevation was 2423 m above sea level, which is low in comparison to the maximum elevation of the collection areas, which ranged from 3,208–4,352 m above sea level.

2.2. Sample Collection and Storage

Streamflow ($n = 123$), tap water ($n = 49$), and composite precipitation ($n = 10$) samples were taken in the Denver area in September 2018 and between March 23, 2019 and October 1, 2019. All samples were immediately placed in an iced cooler for transport to Colorado State University. Samples were kept in a refrigerator at 4°C until sent for analysis.

At the watershed outlets (Figure 1), we sampled streams in well-mixed locations to ensure individual samples were representative of their respective water columns. We took stream samples approximately biweekly when baseflow was present. To ensure only baseflow was captured, we conducted sampling at least three days after precipitation events and examined real-time flow conditions at USGS stream gages for baseflow conditions. However, some streamflow samples may have included stormflow as well as baseflow, as stream hydrographs alone do not indicate water sources. Sampling streams with some amount of stormflow would result in isotopic values closer to recent precipitation events, which may underestimate LIRF contributions. Stream samples were collected in 60 mL clear plastic bottles, filled with no headspace remaining.

It was not feasible to sample sprinklers and leaking pipes directly, and we assumed that both of these sources had the same isotopic signature as tap samples supplied by the common water provider. Tap sampling sites were located in restaurant or gas station bathrooms. Between September 2018 and July 2019, we collected one tap sample per week when streams were sampled close to stream sampling locations. In August 2019, we expanded tap sampling to choose one tap sampling location within each watershed in which we planned to sample baseflow on a given day. We collected cold water when the option was available and occasionally sampled from automatic faucets. Tap samples were collected in the same type of bottles as the stream samples. Twenty-five additional tap water data points in our study area and time period from the [Waterisotopes.org](https://waterisotopes.org) database were included in our analysis (Waterisotopes Database, 2019). Some of the parks in the Denver metropolitan area use raw (untreated) or recycled water (irrigation standard treated

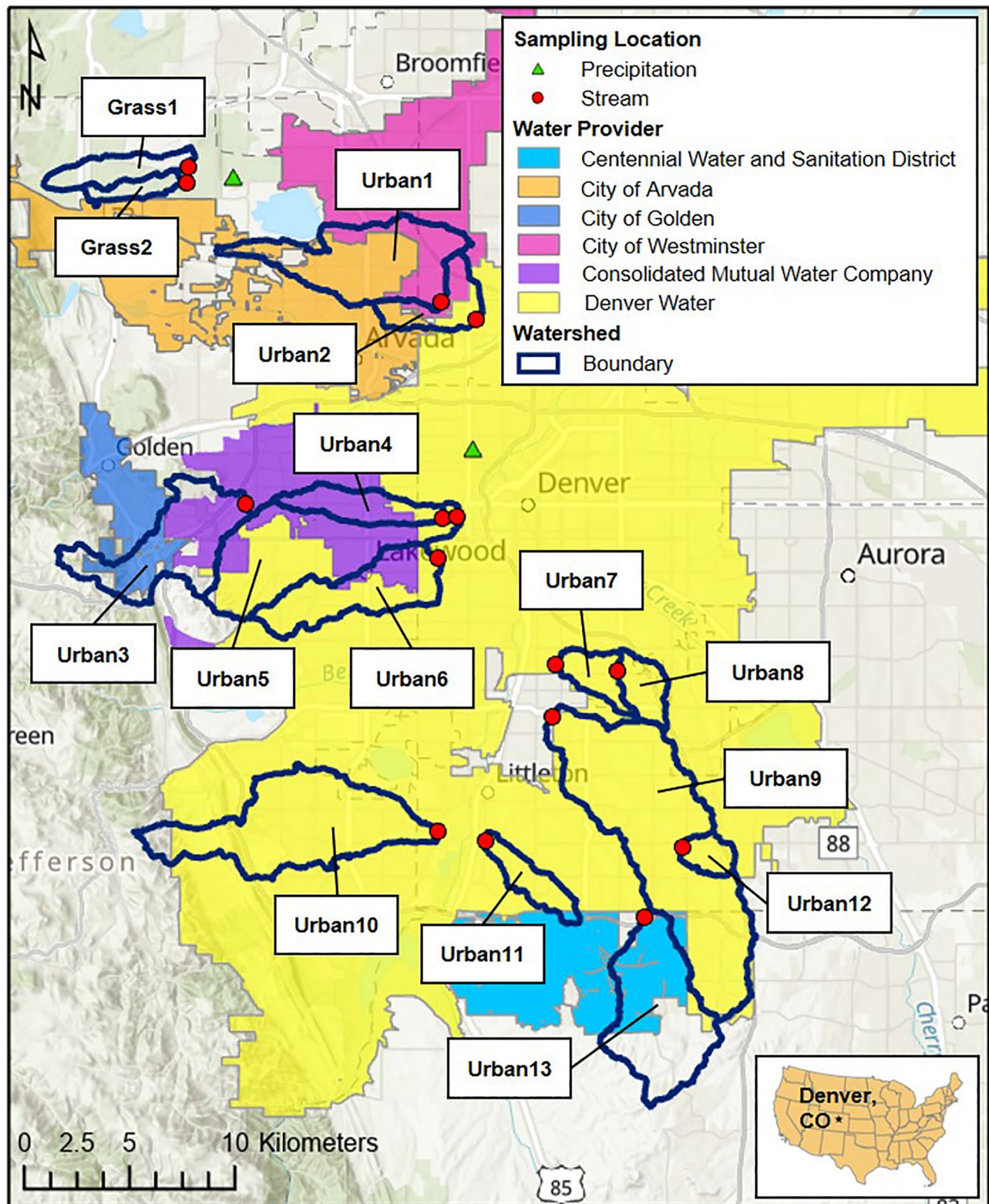


Figure 1. Map of the grassland and urban watersheds, stream sampling locations, precipitation sampling locations, and water provider boundaries in the Denver metropolitan area. Since only the Highlands Ranch Metro District portion of the Centennial Water and Sanitation District service area was considered in the annual water loss reports (Section 2.6), the shapefile for Highlands Ranch Metro District was used to represent the Centennial Water and Sanitation District service area.

Table 1
Watershed Characteristics

ID	Gage authority	Gage ID	Site name	Type	Area (km ²)	Impervious surface cover (%)	Mean elevation (m above sea level)
Grass1	DOE	WOMPOC	Rocky Flats - Woman Creek	Grassland	7.5	5	1,857
Grass2	NA	NA	Rocky Flats - South Woman Creek/Smart Ditch	Grassland	3.7	1	1,842
Urban1	USGS	06719840	Little Dry Creek - Westminster	Urban	28.1	33	1,670
Urban2	USGS	06719845	Little Dry Creek - Federal Blvd.	Urban	36.7	35	1,660
Urban3	USGS	06719560	Lena Gulch - Lakewood	Urban	23.8	24	1,892
Urban4	USGS	06711770	Dry Gulch - Denver	Urban	9.1	42	1,665
Urban5	USGS	06711780	Lakewood Gulch - Denver	Urban	40.7	34	1,718
Urban6	USGS	06711618	Weir Gulch - Denver	Urban	18.6	32	1,690
Urban7	USGS	06711575	Harvard Gulch - Harvard Park	Urban	11.6	32	1,660
Urban8	USGS	06711570	Harvard Gulch - Colorado Blvd.	Urban	5.9	36	1,673
Urban9	USGS	06711555	Little Dry Creek - Englewood	Urban	63.3	29	1,725
Urban10	USGS	06709910	Dutch Creek - Littleton	Urban	38.1	26	1,772
Urban11	USGS	06709740	Lee Gulch - Littleton	Urban	6.5	29	1,696
Urban12	USGS	06711515	Little Dry Creek - Arapahoe	Urban	3.9	44	1,748
Urban13	USGS	06710150	Big Dry Creek - Highlands Ranch	Urban	29.4	22	1,847

Note. Impervious surface cover was based on a supervised land cover model using a random forest classification algorithm in Google Earth Engine using a 1 m resolution 2015 image from the National Agriculture Imagery Program (Fillo, 2020).

wastewater) for irrigation, and we assumed that these sources of water look the same isotopically as the tap water we measured.

Two locations were chosen for sampling of precipitation water-stable isotopes (Figure 1). We followed the Global Network of Isotopes in Precipitation (GNIP) recommendations for precipitation isotope sampling, such as locating precipitation samplers away from large trees or buildings, when establishing sampling sites (GNIP & International Atomic Energy Agency, 2014). The first precipitation sampler was deployed in March 2019, and the second precipitation sampler was deployed in May 2019. The sites were 17.2 km away from each other. Composite (volume-weighted) precipitation samples were collected on a monthly basis. Precipitation was collected in a 3 L plastic bottle using a commercial precipitation isotope sampler (Rain Sampler RS1, Palmex Ltd.). The sampler was designed to prevent evaporation and isotopic fractionation during storage (Palmex, Ltd., 2019). The two precipitation isotope samplers deployed for this study may not have completely captured the variability in Denver's precipitation isotopes. Both samplers were in the

Table 2
Water Providers, Ranges of Mean Elevation in Each Individual Water Source Area Used by the Water Provider (Meters Above Sea Level), Water Sources, and References

Water provider	Mean elevation (masl)	Water sources	References
Denver Water	2,622 m–3,555 m	Williams Fork, Roberts Tunnel, South Platte, Moffat, and Wolford Mountain watersheds	(Leonard Rice Engineers, Inc., 2015)
City of Golden and the City of Westminster	3,036 m	Clear Creek watershed	(City of Golden, 2020; City of Westminster, 2017; USGS, 2020)
City of Arvada	3,556 m	Clear Creek and Moffat	(City of Arvada, 2005; Leonard Rice Engineers, Inc., 2015)
Consolidated Mutual Water Company	2,512 m (Coal Creek)	Clear Creek, Moffat, and Coal Creek watersheds	(Consolidated Mutual Water Company, 2020)
Centennial Water and Sanitation District	2,831 m (South Platte)	South Platte River and deep groundwater	(Leonard Rice Engineers, Inc., 2015)

northern half of the study area (Figure 1), and it was not uncommon for storms to occur in the southern region of the Denver metropolitan area and not in the northern region. Those storms were not included in our precipitation sampling, adding unquantifiable uncertainty to the results for the Urban 7-Urban 13 watersheds. Eight watersheds were wholly or partially within 10 km of a precipitation sampler.

All groundwater wells available for sampling were within agricultural or urban land use areas where there is potential for recharge from irrigation (Musgrove et al., 2014). No wells with only natural, precipitation-driven recharge were available, so groundwater was not sampled. The contribution and timing of recharge from precipitation in this water-limited environment may be naturally minimal based on a nearby rangeland research site (Baffaut et al., 2020).

2.3. Sample Preparation and Analysis

The University of Utah's Stable Isotope Ratio Facility for Environmental Research (SIRFER) laboratory was used for all isotopic analyses. Prior to overnight chilled shipment to the SIRFER laboratory, samples were filtered through 0.2 μm filters into 1.8 mL septa-capped, crimp-sealed glass vials per laboratory specifications (<https://sirfer.utah.edu/oxygen-and-hydrogen-analysis-of-water.html>). We assumed that no isotopic fractionation occurred any time post-sample capture. Samples were analyzed at SIRFER within two months of sample reception using cavity ring-down spectroscopy (L2130-i, Picarro Inc.). Results are reported in the form of an isotope ratio δ relative to the Vienna Standard Mean Ocean Water (VSMOW) standard as

$$\delta \left[\text{‰} \right] = \left(\frac{R_{\text{sample}}}{R_{\text{VSMOW}}} - 1 \right) \times 1000 \quad (1)$$

where R_{sample} and R_{VSMOW} are the $^{18}\text{O}/^{16}\text{O}$ or $^2\text{H}/^1\text{H}$ ratios for $\delta^{18}\text{O}$ and $\delta^2\text{H}$, respectively. The measured reference standard deviation associated with QC for all isotope analysis batches ($n = 37$) were 0.05‰ for $\delta^{18}\text{O}$ and 0.32‰ for $\delta^2\text{H}$.

2.4. General Data Analysis

We compared precipitation isotope measurements against the global meteoric water line (GMWL) (Craig, 1961), local meteoric water line (LMWL) (Harvey, 2005), modeled mean annual precipitation isotope signature, and modeled mean monthly isotope ratios (Bowen, 2020; Bowen et al., 2005; International Atomic Energy Agency, 2015; Welker, 2000). The isotope ratios of our measured samples and the downloaded samples were also compared over time and against watershed characteristics of drainage area, percent imperviousness, elevation, and slope using R (R Core Team, 2019; RStudio Team, 2020). We associated each tap sample with its water provider, and we calculated the percentage of each watershed served by each water provider (Fillo, 2020).

2.5. Two End-Member Mixing Analysis

We used a two end-member mixing analysis to calculate the tap water proportions needed to yield the measured stream isotope value on a given day. Because of the lack of deep groundwater upwelling in our streams, we define one end-member as recent precipitation-derived recharge of shallow groundwater. Henceforth, we term this the “precipitation” end-member. To constrain the appropriate antecedent period prior to stream sampling for this end-member, we analyzed depth-weighted precipitation isotopes from periods of one week to one month, as well as mean annual depth-weighted isotopes. Based on this analysis (results presented in Section 3.5), we concluded that the mean annual precipitation isotopic value was unreasonable, and that the two week antecedent period represented a reasonable proxy for the precipitation end-member.

The tap water end-member was calculated from tap samples associated each watershed within the antecedent period. Tap samples from a specific water provider were associated with a watershed if the provider's service area covered more than one-third of the watershed area. These tap values were then grouped, and the mean, the mean plus one standard deviation, and the mean minus one standard deviation were used to

calculate proportions in the end member mixing model. We did not capture the tap water variation for many water providers throughout the summer, with most of our tap data being taken from Denver Water until August 2019. The isotopic differences among the water providers and temporal variations were larger than anticipated, and a new sampling strategy to better capture this variation was employed starting in August. Limited sampling decreases our ability to draw conclusions about patterns for specific water providers, as has been done with tap water sampling campaigns (Jameel et al., 2016). All streams for which end-member mixing analysis was conducted had watersheds predominantly within the Denver Water service area boundary where we had the greatest data availability.

Stream samples were selected for analysis if (a) six or more associated tap samples were taken within the examined antecedent period prior to the stream sample collection date, (b) the stream isotope value was constrained between the average precipitation and tap isotope values over the antecedent period, and (c) the area-normalized streamflow on the date of isotope sampling was greater than the estimated area-normalized infrastructure loss.

The two end-member mixing analysis required solving the following two equations (Genereux, 1998):

$$f_{precipitation} = \frac{\delta_{tap} - \delta_{stream}}{\delta_{tap} - \delta_{precipitation}} \quad (2)$$

$$f_{tap} = \frac{\delta_{stream} - \delta_{precipitation}}{\delta_{tap} - \delta_{precipitation}} \quad (3)$$

where, $f_{precipitation}$ and f_{tap} were the fractions of precipitation and tap water contributing to streamflow, respectively, and the variables of interest. $\delta_{precipitation}$, δ_{tap} , and δ_{stream} represented the known precipitation, tap, and stream isotope ratios. Mean tap and precipitation isotope values within the antecedent period preceding the stream sample were used to calculate proportions in the end member mixing analysis.

Calculations were performed on the $\delta^2\text{H}$ and $\delta^{18}\text{O}$ isotope values, so each chosen day had two sets of two contribution fractions ($f_{precipitation}$ and f_{tap}). Both sets of contribution fractions were included when determining the overall estimated precipitation and tap contribution ranges to the urban streams. The fractions were multiplied by the area-normalized mean daily streamflow depth to calculate depth contributions from precipitation and tap water to baseflow.

2.6. Tap Contribution Characterization

To estimate the leakage from water distribution infrastructure in each watershed and compare the magnitude to streamflow, we first obtained reports detailing annual infrastructure water losses for each water provider based on the American Water Works Association's Water Audit Software (Colorado Water Conservation Board, 2019). The area considered for the water provider loss reports did not always coincide with the entire service area, so reporting areas were confirmed through personal communication (details given in Fillo, 2020).

The annual loss volumes were divided by the total service area considered in the reports to get area-normalized annual loss depths. These volumes per unit area, or depths, were averaged over 2013–2018 and the annual loss depths were multiplied by the service area coverage proportion(s) for each watershed (provider) and then converted to daily loss depths (loss). We then calculated the proportion of daily loss out of the area-normalized mean daily streamflow:

$$f_{loss} = \frac{\sum_i loss_i * provider_i}{Q} \quad (4)$$

where f_{loss} was the fraction of daily infrastructure loss depth (loss) out of area-normalized mean daily streamflow (Q), where *loss* was averaged over *i* water provider coverage proportions (provider). Then we

calculated the lawn irrigation proportion of streamflow (and uncertainty) by subtracting the daily loss proportion (f_{loss} from Equation 4) from the tap proportion (f_{tap} from Equation 3):

$$f_{\text{irrigation}} = f_{\text{tap}} - f_{\text{loss}} \quad (5)$$

where $f_{\text{irrigation}}$ was the fraction of lawn irrigation contributing to streamflow.

2.7. Uncertainty Analysis

The uncertainty associated with the end-member mixing analysis was calculated using the uncertainty in isotopic analysis and the variation in the isotopic values of the end-members:

$$W_f = \left\{ \left[\frac{f_{\text{precipitation}}}{(\delta_{\text{tap}} - \delta_{\text{precipitation}})} W_{\text{precipitation}} \right]^2 + \left[\frac{f_{\text{tap}}}{(\delta_{\text{tap}} - \delta_{\text{precipitation}})} W_{\text{tap}} \right]^2 + \left[\frac{-1}{(\delta_{\text{tap}} - \delta_{\text{precipitation}})} W_{\text{stream}} \right]^2 \right\}^{\frac{1}{2}} \quad (6)$$

where W_f represented the 70% confidence limits for uncertainty associated with $f_{\text{precipitation}}$ and f_{tap} , and $W_{\text{precipitation}}$, W_{tap} , and W_{stream} represented the calculated uncertainty associated with the precipitation, tap, and stream samples, respectively (Genereux, 1998). The uncertainty for the precipitation and tap isotope end-members was calculated by multiplying the standard deviation of the individual samples representing the endmembers (see criteria in Section 2.5 to associate tap and precipitation samples with a stream sample) by the associated 70% t-value (Genereux, 1998). We could not use the standard deviation of stream samples in the end-member mixing analysis as we did not group stream samples, so instead used half the analytical precision multiplied by the associated 70% t-value to represent the uncertainty in the stream isotopic value (as in Genereux, 1998).

The uncertainty associated with the characterization of tap water as lawn irrigation or infrastructure loss was based on the temporal variability in infrastructure loss values. The 70% uncertainty (W_{loss}) in infrastructure loss was calculated by multiplying the standard deviation in infrastructure loss over 2013–2018 by the 70% t-value. The uncertainty associated with the lawn irrigation proportion was calculated using uncertainty propagation:

$$W_{\text{irrigation}} = \left[(W_{\text{loss}})^2 + (W_f)^2 \right]^{\frac{1}{2}} \quad (7)$$

where $W_{\text{irrigation}}$ refers to the uncertainty associated with the estimated fraction of lawn irrigation contributing to streamflow and W_{loss} refers to the calculated 70% uncertainty associated with the infrastructure loss estimates. Each uncertainty was calculated separately and may exceed its associated endmember proportion estimate (e.g., $W_{\text{precipitation}}$ is not bounded by $f_{\text{precipitation}}$).

There were other sources of uncertainty that could not be directly quantified, such as the spatial variability in infrastructure loss over a water provider area, temporal variability in infrastructure loss at timescales smaller than annual, the fraction of infrastructure loss that contributed to the stream, and the variability in precipitation and tap isotopic values beyond the spatial and temporal scales over which data were collected. Without the necessary information on spatially distributed and temporal variability in infrastructure loss, we assumed the infrastructure loss contributions were uniform across the service area and throughout the year. We also assumed that infrastructure loss was equal to infrastructure leakage, which all contributed to streamflow. This led to the criterion (c) used for stream sample analysis, that the area-normalized streamflow on the date of isotope sampling was greater than the estimated area-normalized infrastructure loss, so that the contribution from infrastructure loss to streamflow could not exceed total streamflow. However, infrastructure loss also included unauthorized use, inaccurate metering (Karamouz et al., 2010), and leakage that becomes evapotranspiration, which would not contribute to streamflow. We did not have estimates of these components of infrastructure loss and therefore used infrastructure loss as an estimate for infrastructure leakage. There were two stream samples out of 102 (Urban 8 on September 4, 2019 and Urban 11 on September 30, 2019) in which the area-normalized infrastructure loss was greater than the area-normalized streamflow on that date, meaning that in these cases our estimate of infrastructure loss contributions to the

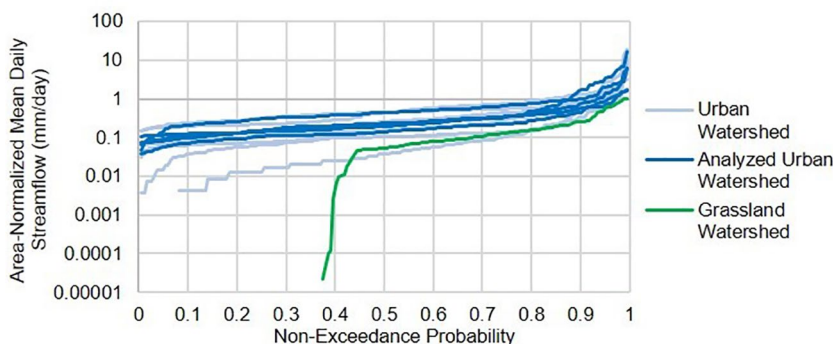


Figure 2. Nonexceedance probabilities for area-normalized mean daily streamflow in the Denver metropolitan area. Zero flow and unreported flow days are not shown on the logarithmic y-axis. Time frame is April 1, 2019–September 30, 2019. Analyzed Urban Watersheds indicates the subset of watersheds presented in Figure 6.

stream were clearly overestimated. We also assumed other potential sources of tap water, such as leakage from wastewater pipes and soil-wetting for land development, were negligible.

3. Results

3.1. Streamflow Comparison

Analysis of mean daily streamflow in the Denver metropolitan area revealed that there were major differences in the nonexceedance probability curves of urban and grassland streamflow in the summer (April–September) of 2019 (Figure 2). The only gaged grassland stream was dry for almost 40% of the summer, while urban streams were dry for less than 10% of the summer. Eleven out of 13 urban streams had perennial flow. When there was flow present in the grassland stream, the area-normalized flow was overall lower than the urban streamflow across the nonexceedance probability curve. The urban streams that were used in our end-member mixing analysis (chosen based on the criteria in Section 2.5) were in the same streamflow range as other urban streams in the Denver region (Figure 2).

3.2. Water-Stable Isotope Relationships

Comparing isotope measurements to the GMWL and LMWL can provide insight into local hydrologic systems. Deviation from the GMWL is not uncommon, and points plotting below the GMWL can indicate that the sampled water underwent evaporative processes (Kendall & McDonnell, 1999). Our measured precipitation isotope values plotted on the GMWL in April and May, but dropped below it in June 2019 and remained below the GMWL through September 2019 (Figure 3a). Since the Denver metropolitan area has a semi-arid climate, this observation was not unexpected. However, comparison to a LMWL created using water-stable isotope data from the northeastern plains of Colorado (slope of 7.9) suggested that our precipitation measurements were at times below both the LMWL and GMWL (Harvey, 2005). The precipitation isotope values for both sites plotted along a similar curve during summer 2019, but the isotope values were never identical in the same month (Figure 3a). Neither site consistently yielded higher precipitation isotope values compared to the other.

Tap and surface water $\delta^2\text{H}$ and $\delta^{18}\text{O}$ values plotted below the GMWL earlier in the year than did precipitation (Figure 3). There was a consistent slope of the tap (7.0) and surface water (6.9) samples throughout the summer and to each other, indicating the relationship between $\delta^2\text{H}$ and $\delta^{18}\text{O}$ was fairly stable among both sample types despite increases and decreases in the isotope values themselves (Figures 3b and 3c). The tap isotope values were similar to the stream isotope values for a given month and had a more negative and narrow range compared to precipitation values. The most negative isotope values were observed in the spring (March–June) and late summer (August–September), and the least negative isotope values were observed in July and parts of August (Figure 3).

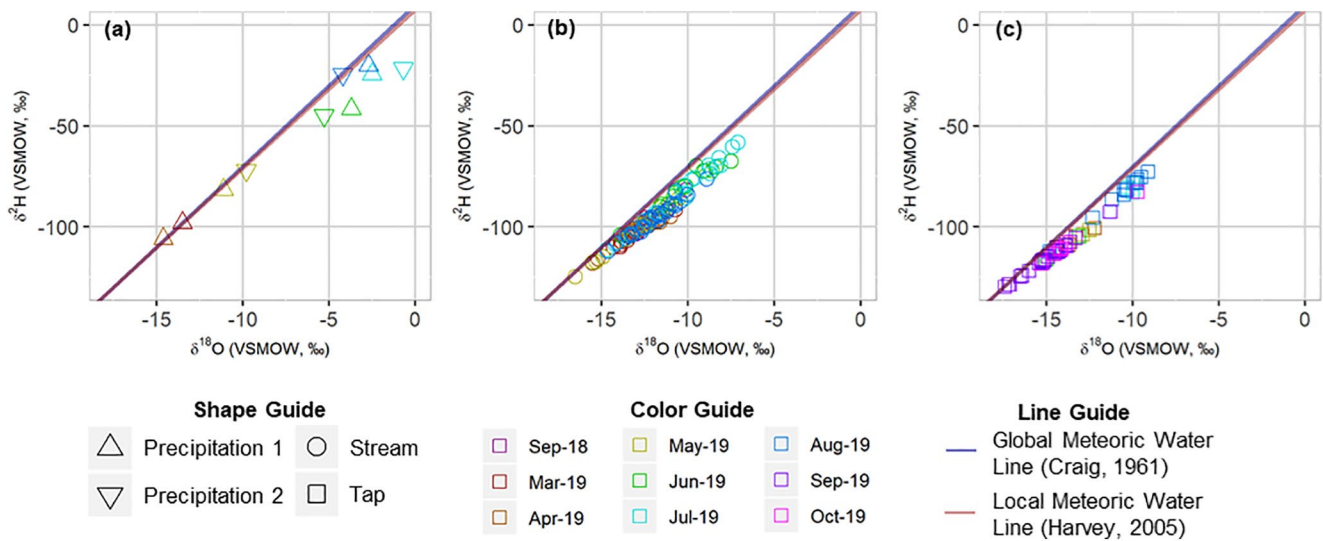


Figure 3. Temporal variation in ratios of $\delta^2\text{H}$ to $\delta^{18}\text{O}$ in (a) precipitation with both precipitation sampling sites shown (Precipitation 1 and Precipitation 2) (b) surface water and (c) tap water.

3.3. Changes in Isotope Values Over Time

Temporal and spatial variation was observed across all sample types and watersheds (Figure 4). Precipitation isotope values plotted along an increasing s-shaped curve between April and September, while the tap and stream samples were fairly constant throughout the sampling period with a higher excursion in July and August. Most urban stream, grassland stream, and tap isotope values plotted relatively close to the precipitation curves until early June, but two urban streams within the Consolidated Mutual Water Company service area plotted below the precipitation curve (Figures 4f and 4g). By July 2019, the grassland streams were no longer flowing and almost all urban stream and tap measurements displayed less negative isotope values. Stream and tap isotope values then dropped well below the precipitation curve in late August and remained low through the rest of the study period. Stream values were between the precipitation curve and the tap scatter or within the tap scatter at the end of the summer, with the sole exception of Urban13 on September 30, 2019 (Figure 4o). No relationships could be established between isotope values and watershed characteristics such as drainage area, percent imperviousness, elevation, watershed slope, or dominant water providers.

3.4. Tap Water Variation

The tap water in the Denver metropolitan area displayed substantial isotopic variation across providers and over time (Figure 5). Samples from all water providers had the least negative isotope values in July and early August, at the same time as the stream samples were least negative (Figures 4 and 5). Tap samples taken on or around the same day within a single water provider had $\delta^2\text{H}$ values that varied up to 19‰ and were most variable in Centennial Water and Sanitation District that used both surface and groundwater sources. More tap samples were taken between August 2019 and October 2019 because we altered our tap sampling strategy to better capture the variation within and between water providers. The isotope values of Consolidated Mutual Water Company, Denver Water, and the City of Westminster were similar on the same day, but the City of Arvada's and Centennial Water and Sanitation District's means were lower and higher, respectively. Despite the observed variation across and within water providers (Figure 5), a substantial difference between late summer (September 2019) tap samples and local precipitation is apparent (Figure 4).

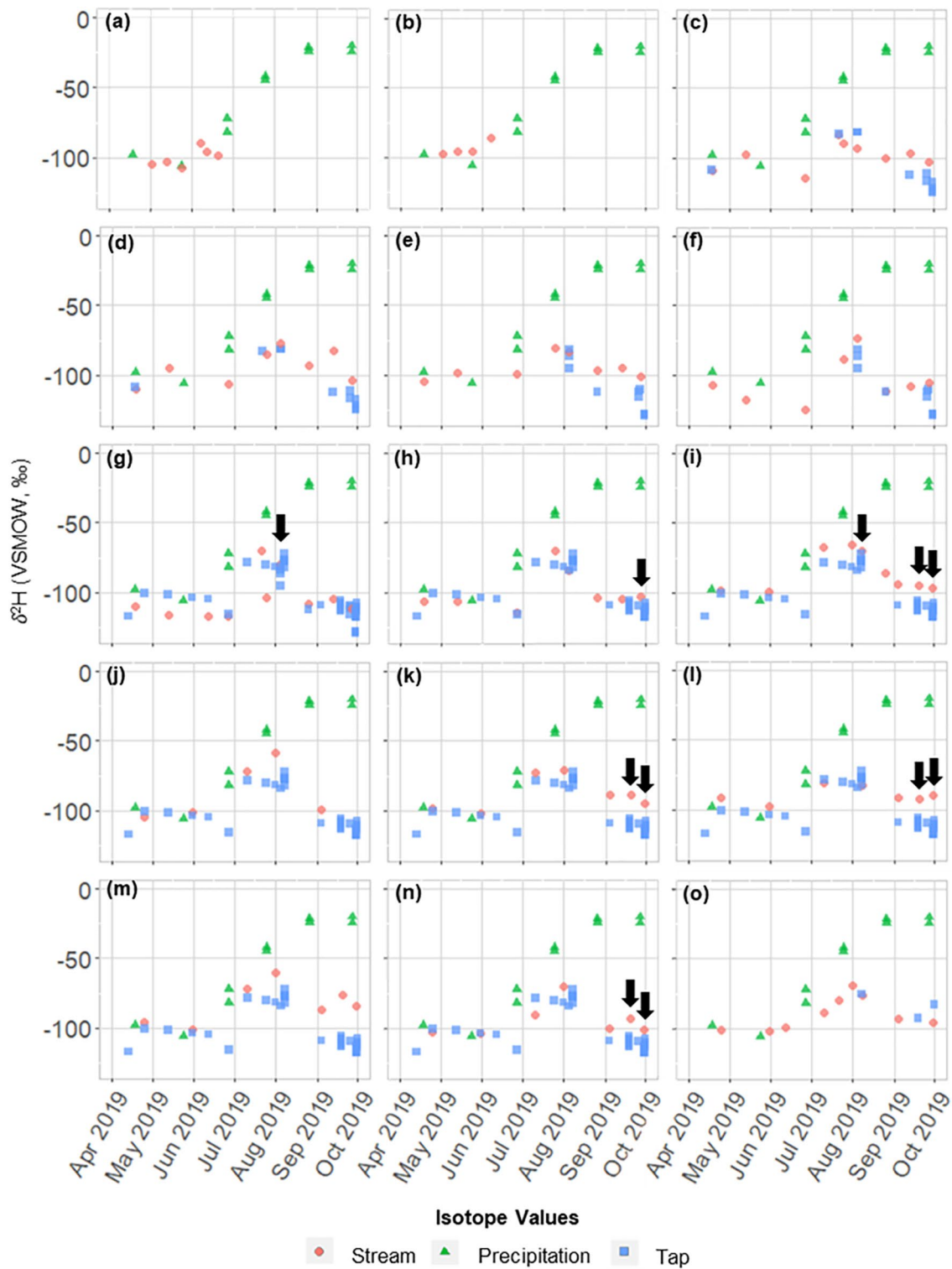


Figure 4. Changes in $\delta^2\text{H}$ over time for watersheds (a) Grass1, (b) Grass2, (c) Urban1, (d) Urban2, (e) Urban3, (f) Urban4, (g) Urban5, (h) Urban6, (i) Urban7, (j) Urban8, (k) Urban9, (l) Urban10, (m) Urban11, (n) Urban12, and (o) Urban13. Samples taken in September 2018 were not plotted due to temporal separation from the rest of the samples. Arrows indicate dates analyzed in Figure 6. Analytical uncertainty is smaller than the symbol size.

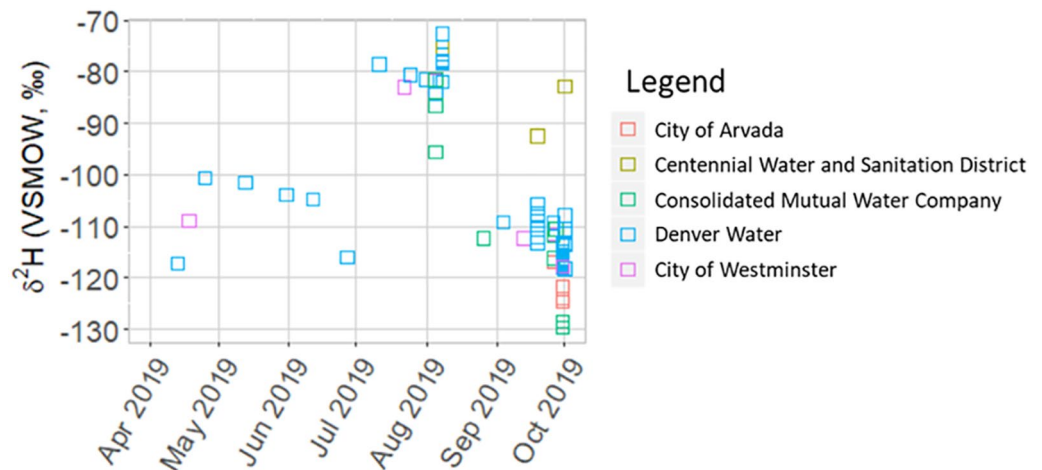


Figure 5. Changes in $\delta^2\text{H}$ over time for different tap water providers.

3.5. Flow Contribution Analysis

Eleven samples in six streams were chosen for the flow contribution estimation as per the criteria outlined in Section 2.5 (indicated by arrows in Figure 4). Tap contributions (infrastructure loss and lawn irrigation combined) dominated streamflow on all analyzed days and ranged from $65\% \pm 10\%$ – $93\% \pm 3\%$ of streamflow (Figures 6a and 6b). Across both isotopes, the mean tap contribution was 80%, with similar results from $\delta^2\text{H}$ and $\delta^{18}\text{O}$ (Figures 6a and 6b). The daily streamflow depths attributed to tap sources ranged from $5.7 \times 10^{-2} \text{ mm} \pm 7.6 \times 10^{-3} \text{ mm}$ to $3.9 \times 10^{-1} \text{ mm} \pm 1.7 \times 10^{-2} \text{ mm}$, with a mean of $1.9 \times 10^{-1} \text{ mm}$. High tap water percent contributions (Figures 6a and 6b) did not always coincide with high streamflow depths (Figures 6c and 6d).

We assumed the total tap contribution was made up of lawn irrigation and infrastructure loss contributions. All analyzed watersheds had similar area-normalized infrastructure daily loss depths, ranging from $3.2 \times 10^{-2} \text{ mm} \pm 1.2 \times 10^{-2} \text{ mm}$ to $3.3 \times 10^{-2} \text{ mm} \pm 1.2 \times 10^{-2} \text{ mm}$ (Figures 6c and 6d). The similarity across watersheds was because all analyzed watersheds were within the Denver Water or Consolidated Mutual Water Company service areas and our infrastructure loss estimates were constant within a single water provider.

LIRF accounted for $32\% \pm 10\%$ – $82\% \pm 21\%$ of daily streamflow, with a mean of 59%, once the estimated contribution from infrastructure loss is separated from the tap water contribution. The LIRF daily flow depths ranged from $2.5 \times 10^{-2} \text{ mm} \pm 7.6 \times 10^{-3} \text{ mm}$ to $3.6 \times 10^{-1} \text{ mm} \pm 1.8 \times 10^{-2} \text{ mm}$. Greater flow depths are attributed to lawn irrigation on dates with higher streamflow. This occurred because infrastructure loss was assumed constant across dates, most streams had similar loss contributions, and the split between the tap and precipitation contribution fraction were not strongly related to streamflow depth. We did not find significant relationships between streamflow contributions and watershed characteristics.

We also conducted the end-member mixing analysis with one-month, two week, and one-week antecedent periods with requirements of at least two or at least six tap samples within that antecedent window (Tables S1–S6). While the mean transit time through these watersheds is unknown and may vary by watershed, we used relatively short antecedent periods as urbanization shortens transit times (Soulsby et al., 2014). The mixing analysis using just two or more tap samples taken within the antecedent period had large uncertainties in the tap contribution fraction because of the temporal variability of the isotopic composition of the tap water from a single water provider (Figure 5).

End-member mixing analyses requiring at least six tap samples within the antecedent window yielded overall similar results for eight stream samples analyzed for all of the antecedent windows (Table S7). The difference in tap percentage contributions across antecedent windows was generally less than 1% for $\delta^2\text{H}$ and

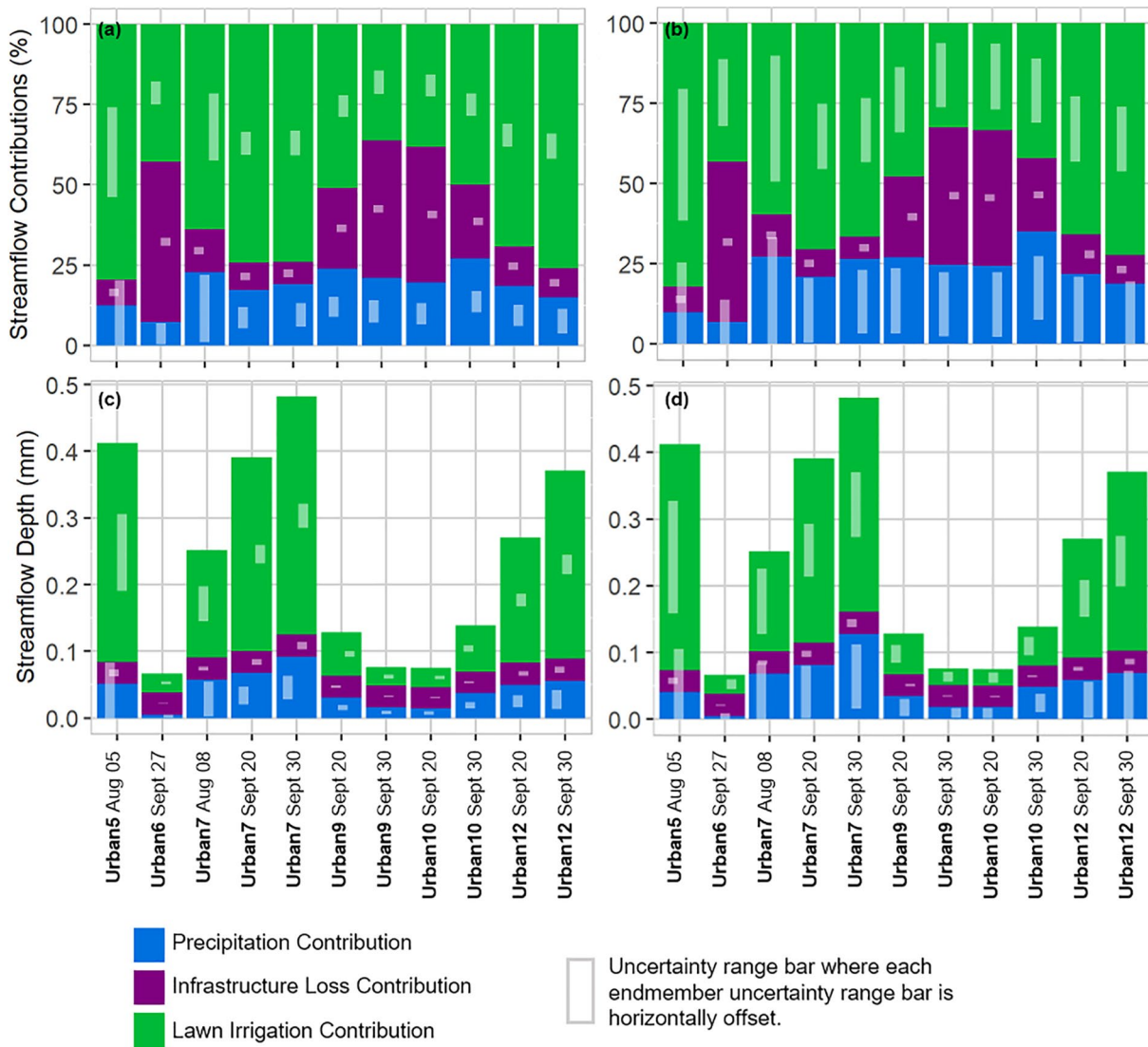


Figure 6. Precipitation, infrastructure loss, and lawn irrigation contributions to streamflow as (a) percentages of total baseflow calculated using $\delta^2\text{H}$, (b) percentages of total baseflow calculated using $\delta^{18}\text{O}$, (c) streamflow depths calculated using $\delta^2\text{H}$, and (d) streamflow depths calculated using $\delta^{18}\text{O}$ in select streams on specific days. The uncertainty range bars are centered on the midpoint of the associated endmember contribution. The uncertainty range bar heights show the uncertainty in the associated endmember based on Equations 6 and 7. For example, the uncertainty range bar height for precipitation in panels (a and b) extends from $(f_{\text{precip}} * 100/2) \pm W_{\text{precip}} * 100$. Note: X-axis displaying analyzed streams and dates (all in 2019) applies to both sets of graphs.

5% for $\delta^{18}\text{O}$, with the exception of the August 8 sample where the variation in the precipitation end-member over the antecedent period led to a range of up to 14% (Table S7). The uncertainty was higher for the precipitation fraction for the one-month antecedent period, and the one-week antecedent period had fewer stream sampling dates ($n = 8$) that had six or more tap samples taken in the associated water provider's service area in the previous week. Therefore, all subsequent flow contributions presented were based on the end-member mixing analysis criteria of a two-week antecedent period.

If precipitation contributions to the stream were mixed with groundwater with longer travel times, the isotopic values should have begun to resemble Denver's mean annual precipitation depth-weighted isotope values ($\delta^2\text{H} = -82.8\text{‰}$, $\delta^{18}\text{O} = -11.2\text{‰}$) (Bowen, 2020; Bowen et al., 2005; International Atomic Energy Agency, 2015; Welker, 2000). If this were the case, stream isotope values in July 2019 and August 2019 would be higher than both the precipitation-recharged groundwater and tap end members (Figure 4). Late August 2019 and September 2019 values for analyzed watersheds could have been a mixture of precipitation-re-

charged groundwater and tap samples, but the tap proportions would be smaller than calculated here for the mixture of precipitation and tap water (Figure 4).

4. Discussion

4.1. Tap Contributions to Urban Baseflow

There was flow in the urban streams longer than the grassland stream during the 2019 summer (Figure 2), consistent with data from other years (Fillo, 2020). Channel incision and vegetation removal have been suggested as causes of increased groundwater flux into post-development rivers in semi-arid climates (Hibbs et al., 2012), but if this were the only cause of increased baseflow in the Denver metropolitan area, we would expect both the urban and grassland streams to have isotope values similar to recent local or mean annual precipitation isotopes. Grassland stream isotopes did plot with the recent precipitation isotopes while there was flow (Figures 4a and 4b), as did the urban streams in the spring and early summer. However, after July 2019, the urban stream values frequently were more negative than the precipitation values (Figure 4c through Figure 4o). Based on these isotopic differences, higher urban streamflow in the Denver metropolitan area cannot be solely attributed to increased flux of precipitation-recharged groundwater.

Urbanization can also increase baseflow by introducing new sources of water to the hydrologic system, such as tap water. Because none of the studied streams received wastewater effluent, we identified two likely sources of additional water: infrastructure leakage and lawn irrigation. Both infrastructure leakage and lawn irrigation come from tap sources and have been shown to significantly contribute to urban recharge in dry climates (Lerner, 2002). The dominant input of tap water was confirmed by stream isotope values plotting closer to the tap water isotopes than the precipitation isotopes, most notably from July 2019 through September 2019 (Figure 4). Our end-member mixing analysis results reflected this tendency, with baseflow sourced dominantly from tap water (Figures 6a and 6b). Much of the summer baseflow in the Denver metropolitan area can thus be attributed to tap water sources.

4.2. Infrastructure Leakage and Lawn Irrigation Contributions to Urban Baseflow

Approximately $5\% \pm 1.3\%$ of Denver's annual water distribution was considered "loss" in the 2013–2018 Denver Water reports (Colorado Water Conservation Board, 2019). This loss percentage is comparable to other semi-arid cities in the United States such as Los Angeles (6%–8%) (Garcia-Fresca & Sharp, 2005). The infrastructure loss flow rate for the analyzed watersheds, $3.2 \times 10^{-2} \text{ mm} \pm 1.2 \times 10^{-2} \text{ mm}$, was low in comparison to reported infrastructure loss rates for humid subtropical cities in the United States. Studies conducted in Baltimore, Maryland, USA and Austin, Texas, USA reported area-normalized infrastructure loss estimates of $4.3 \times 10^{-1} \text{ mm/day}$ and a range of $7.0 \times 10^{-2} \text{ mm/day}$ – $3.2 \times 10^{-1} \text{ mm/day}$, respectively (Bhaskar & Welty, 2012; Garcia-Fresca & Sharp, 2005).

4.3. Assumptions and Limitations

Our ability to describe the isotopic behavior of Denver's precipitation was also limited by taking composite monthly samples. When comparing our precipitation results to modeled mean monthly precipitation values (Bowen, 2020; Bowen et al., 2005; International Atomic Energy Agency, 2015; Welker, 2000), our measured precipitation isotopes were more negative from April 2019 - June 2019 and less negative from July 2019–September 2019 (Figure 3). The large deviation of our measured precipitation points from the GMWL and LMWL indicates that precipitation was subject to evaporative fractionation within our July 2019–September 2019 samples (Figure 3). This may be due to below cloud evaporation, as is more common in inland, arid environments (Wang et al., 2016) or evaporation from precipitation samplers post-collection, although these samplers were designed to prevent post-collection evaporation (Palmex, Ltd., 2019). Nonetheless, the large difference between late summer precipitation and stream isotopes ($>30\text{‰}$ for $\delta^2\text{H}$ and $>4\text{‰}$ for $\delta^{18}\text{O}$), and the agreement of stream and tap isotopes suggest that inadequate sampling of precipitation is unlikely to explain the observed stream isotope values.

We assumed no isotopic fractionation occurred between the sprinkler or leakage point and the urban stream and that there was not significant in-stream evaporation. The similarity of slopes of the $\delta^2\text{H}$ - $\delta^{18}\text{O}$ relationships for tap and stream samples supports this assumption and suggests that there was not likely to be significant evaporation between tap and stream (Figure 3), as does previous research comparing runoff from lawn irrigation to tap sources (Clifford & Hibbs, 2020). Stream sample deuterium-excess values were largely bounded between precipitation and tap isotopic values (Figure S1), indicating that the variation in stream isotopic values can largely be explained by mixing between these end-members and not evaporation. There was a small difference in contribution estimates between $\delta^2\text{H}$ and $\delta^{18}\text{O}$ of 3.6% (Figure S2), also indicating a minor role of evaporative fractionation in-stream. In two samples, (Urban 5 on September 27, 2019 and Urban 10 on August 8, 2019), stream isotope values for both $\delta^2\text{H}$ and $\delta^{18}\text{O}$ were more negative than the tap values sampled, indicating we were missing another possible, more negative contributor to baseflow, such as earlier piped water, older precipitation-sourced shallow groundwater, or deeper groundwater.

4.4. Implications and Future Work

There are substantial contributions from tap sources to late summer (August–September) baseflow in the Denver metropolitan area. The prevalence of LIRF in Denver streams varies between watersheds, and the largest lawn irrigation contributions occur in streams with the highest area-normalized mean daily streamflow. Increases in baseflow and stream permanence have cascading implications for stream ecology (Bhaskar, Beesley, et al., 2016; Bunn & Arthington, 2002; Reich et al., 2010; Riley et al., 2005). During dry periods in semi-arid cities, nutrient pollution from lawn fertilizers and wastewater effluent in urban baseflow can be substantial and may exceed the load from stormwater (McPherson et al., 2005; Stein & Ackerman, 2007; Toor et al., 2017).

Tap water contributing most of the water to urban streams on sunny days is problematic from a water use efficiency perspective, since this water was applied for landscape plant growth. However, in the context of a water rights perspective, transbasin tap water that returns to urban streams can be claimed as a return flow credit that allows municipalities to withdraw the equivalent amount upstream. Many Front Range, Colorado municipalities claim 15% of the lawn irrigation application rate as a return flow credit (Oad & Dispigno, 1997). Our estimates found that lawn irrigation inputs were present in Denver's urban streams, and the contributions varied by watershed. The daily flow depth range for LIRF (2.5×10^{-2} mm \pm 7.6×10^{-3} mm to 3.6×10^{-1} mm \pm 1.8×10^{-2} mm) spanned one order of magnitude. This range is low in comparison to the 2.2 mm/day irrigation application estimates in nearby Aurora, Colorado (Gage & Cooper, 2015). Some water applied for irrigation purposes will be taken up by plants, so the LIRF to the streams should be lower than the application rate. Using a lawn irrigation application rate of 2.2 mm/day and the LIRF daily flow depths, approximately 1% \pm 0.3%–16% \pm 0.8% of irrigation applied reaches urban streams in the Denver metropolitan area. Although these estimates are based on an average irrigation rate from one municipality in the Denver region, this analysis suggests that consumers in the Denver metropolitan area may not always be contributing 15% as LIRF.

Our research spanned a single summer, so future work is needed to understand the broader patterns of the roles that tap water and lawn irrigation play in semi-arid, urban streams over multiple years with variable climate and over more watersheds. Future work using water-stable isotope analysis or other geochemical tracers (Beal et al., 2020; Kaushal & Belt, 2012) of tap water would benefit from longer temporal scales and greater capture of precipitation and subsurface signatures, and is complemented by work on the plot scale investigating the movement of irrigated water into residential soil and uptake by trees and lawns (Gómez-Navarro et al., 2019; Litvak et al., 2017; Oerter & Bowen, 2017). Greater temporal and spatial resolution of infrastructure leakage also will further constrain the contributions from lawn irrigation as a subset of overall tap water contributions. Identifying the contributions of specifically lawn irrigation to streamflow will be increasingly important as municipalities respond to water scarcity with short-term drought conservation measures and longer-term efficiency in urban irrigation.

5. Conclusions

To improve water resource conservation in water-scarce cities, greater knowledge of the role of lawn irrigation on urban streamflow is needed. We aimed to estimate the contributions from (a) tap water and (b) lawn irrigation to summertime Denver-area baseflow with water-stable isotopes ($\delta^2\text{H}$ and $\delta^{18}\text{O}$). Urban stream, grassland stream, tap, and precipitation isotope samples were taken and analyzed in September 2018 as well as from March 2019 through October 2019 (Figure 3). A two end-member mixing analysis with a two-week antecedent window was used to estimate the contributions of tap water and local precipitation to urban baseflow based on the $\delta^2\text{H}$ and $\delta^{18}\text{O}$ values from select days (Figure 4). The lawn irrigation component to baseflow was calculated by subtracting reported water distribution infrastructure losses from the overall tap contribution to baseflow.

1. How much of Denver's summertime baseflow comes from tap water sources? We found that tap water made up the majority ($65\% \pm 10\%$ – $93\% \pm 3\%$, with a mean of 80%) of urban baseflow in all analyzed days and the contribution depth range was $5.7 \times 10^{-2} \text{ mm} \pm 7.6 \times 10^{-3} \text{ mm}$ to $3.9 \times 10^{-1} \text{ mm} \pm 1.7 \times 10^{-2} \text{ mm}$ (Figure 6).
2. How much of the tap water contribution can be attributed to lawn irrigation compared to other sources of tap water?
Lawn irrigation comprised $32\% \pm 10\%$ – $82\% \pm 21\%$ with a mean of 59% of the flow in our watersheds and contributed flow depths ranging from $2.5 \times 10^{-2} \text{ mm} \pm 7.6 \times 10^{-3} \text{ mm}$ to $3.6 \times 10^{-1} \text{ mm} \pm 1.8 \times 10^{-2} \text{ mm}$ (Figure 6).

Useful areas for future work include characterizing the isotopic behavior of baseflow across space using more explanatory landscape characteristics and in water-scarce cities over multiple years to better understand the long-term effects urbanization has had on hydrology across cities and climates.

Data Availability Statement

The data used in this analysis are available in CUAHSI HydroShare (<http://www.hydroshare.org/resource/88bff690c1494e14a7ef90047eeff34a>) and in Fillo (2020).

Acknowledgments

Wyatt Young, Connor Williams, Shannon Petts, Ben Choat, Katie Knight, and Ryan Baird assisted with sample collection. The authors appreciate helpful comments from Stephanie Kampf, Ryan Bailey, Rose Smith, Gabe Bowen, and anonymous reviewers. This work was partially supported by the USDA National Institute of Food and Agriculture, Hatch project 1015939 and NSF 2045340.

References

- Baffaut, C., Baker, J. M., Biederman, J. A., Bosch, D. D., Brooks, E. S., Buda, A. R., et al. (2020). Comparative analysis of water budgets across the U.S. long-term agroecosystem research network. *Journal of Hydrology*, 588, 125021. <https://doi.org/10.1016/j.jhydrol.2020.125021>
- Barron, O. V., Froend, R., Hodgson, G., Ali, R., Dawes, W., Davies, P., & McFarlane, D. (2013). Projected risks to groundwater-dependent terrestrial vegetation caused by changing climate and groundwater abstraction in the Central Perth Basin, Western Australia. *Hydrological Processes*, 5513–5529. <https://doi.org/10.1002/hyp.10014>
- Beal, L., Senison, J., Banner, J., Musgrove, M., Yazbek, L., Bendik, N., et al. (2020). Stream and spring water evolution in a rapidly urbanizing watershed, Austin, TX. *Water Resources Research*, 56, e2019WR025623. <https://doi.org/10.1029/2019WR025623>
- Berg, A., Byrne, J., & Rogerson, R. (1996). An Urban Water Balance Study, Lethbridge, Alberta: Estimation of Urban Lawn Overwatering And Potential Effects On Local Water Tables. *Canadian Water Resources Journal*, 21(4), 355–365. <https://doi.org/10.4296/cwrj2104355>
- Bhaskar, A. S., Beesley, L., Burns, M. J., Fletcher, T. D., Hamel, P., Oldham, C. E., & Roy, A. H. (2016). Will it rise or will it fall? Managing the complex effects of urbanization on base flow. *Freshwater Science*, 35(1), 293–310. <https://doi.org/10.1086/685084>
- Bhaskar, A. S., Hogan, D. M., & Archfield, S. A. (2016). Urban base flow with Low Impact Development. *Hydrological Processes*, 30(18), 3156–3171. <https://doi.org/10.1002/hyp.10808>
- Bhaskar, A. S., & Welty, C. (2012). Water balances along an urban-to-rural gradient of metropolitan Baltimore, 2001–2009. *Environmental & Engineering Geoscience*, 18(1), 37–50. <https://doi.org/10.2113/gsegeosci.18.1.37>
- Bijoor, N. S., Pataki, D. E., Haver, D., & Famiglietti, J. S. (2014). A comparative study of the water budgets of lawns under three management scenarios. *Urban Ecosystems*, 17(4), 1095–1117. <https://doi.org/10.1007/s11252-014-0361-4>
- Bowen, G. J. (2020). *Gridded maps of the isotopic composition of meteoric waters*. Retrieved from <http://www.waterisotopes.org>
- Bowen, G. J., Wassenaar, L. I., & Hobson, K. A. (2005). Global application of stable hydrogen and oxygen isotopes to wildlife forensics. *Oecologia*, 143(3), 337–348. <https://doi.org/10.1007/s00442-004-1813-y>
- Bunn, S. E., & Arthington, A. H. (2002). Basic principles and ecological consequences of altered flow regimes for aquatic biodiversity. *Environmental Management*, 30(4), 492–507. <https://doi.org/10.1007/s00267-002-2737-0>
- Christian, L. N., Banner, J. L., & Mack, L. E. (2011). Sr isotopes as tracers of anthropogenic influences on stream water in the Austin, Texas, area. *Chemical Geology*, 282(3–4), 84–97. <https://doi.org/10.1016/j.chemgeo.2011.01.011>
- City and County of Denver. (2019). *Denver open data Catalog*. August 20, 2020. Retrieved from <https://www.denvergov.org/opendata>
- City of Arvada. (2005). *Water sources, treatment, and distribution*. Retrieved from <https://www.arvada.org/residents/services-and-sustainability/water-sourcetrement-and-distribution>
- City of Golden. (2020). *Water supply*. Retrieved from <https://www.cityofgolden.net/government/departments-divisions/water/water-supply/>

- City of Westminster. (2017). *Where does your drinking water come from?* Retrieved from <https://www.cityofwestminster.us/News/where-does-your-drinking-water-come-from>
- Clifford, G., & Hibbs, B. (2020). Evaluation of Water Isotopes and Nutrient Loading in Urban Runoff at a Southern California Residential Site. *World Environmental and Water Resources Congress 2020*, 10–19. <https://doi.org/10.1061/9780784482964.002>
- Colorado Water Conservation Board. (2019). *Water efficiency data portal*. Retrieved from <http://www.cowaterefficiency.com/>
- Consolidated Mutual Water Company. (2020). *Service area map*. Retrieved from <https://www.cmwc.net/about-us/service-area-map/>
- Cooley, H., Phurisamban, R., & Gleick, P. (2019). The cost of alternative urban water supply and efficiency options in California. *Environmental Research Communications*, 1(4), 042001. <https://doi.org/10.1088/2515-7620/ab22ca>
- Craig, H. (1961). Isotopic Variations in Meteoric Waters. *Science*, 133(3465), 1702–1703. <https://doi.org/10.1126/science.133.3465.1702>
- Dennehy, K. F., Litke, D. W., Tate, C. M., & Heiny, J. S. (1993). South Platte River Basin - Colorado, Nebraska, and Wyoming. *Journal of the American Water Resources Association*, 29(4), 647–683. <https://doi.org/10.1111/j.1752-1688.1993.tb03231.x>
- DeOreo, W. B., Mayer, P. W., Dziegielewski, B., Kiefer, J., & Water Research Foundation. (2016). *Residential end uses of water, version 2*. Denver, CO: Water Research Foundation. Retrieved from <http://www.waterrf.org/Pages/Projects.aspx?PID=4309>
- de Wet, R. F., West, A. G., & Harris, C. (2020). Seasonal variation in tap water $\delta^2\text{H}$ and $\delta^{18}\text{O}$ isotopes reveals two tap water worlds. *Scientific Reports*, 10(1), 13544. <https://doi.org/10.1038/s41598-020-70317-2>
- Ehleringer, J. R., Barnette, J. E., Jameel, Y., Tipple, B. J., & Bowen, G. J. (2016). Urban water – A new Frontier in isotope hydrology. *Isotopes in Environmental and Health Studies*, 52(4–5), 477–486. <https://doi.org/10.1080/10256016.2016.1171217>
- Fillo, N. K. (2020). *Quantifying lawn irrigation contributions to semi-arid, urban stream baseflow with water-stable isotopes (M.S. Thesis)*. Colorado State University. Fort Collins, CO. Retrieved from <https://hdl.handle.net/10217/208469>
- Gabor, R. S., Hall, S. J., Eiriksson, D. P., Jameel, Y., Millington, M., Stout, T., et al. (2017). Persistent urban influence on surface water quality via impacted groundwater. *Environmental Science & Technology*, 51(17), 9477–9487. <https://doi.org/10.1021/acs.est.7b00271>
- Gage, E., & Cooper, D. J. (2015). The influence of land cover, vertical structure, and socioeconomic factors on outdoor water use in a western US City. *Water Resources Management*, 29(10), 3877–3890. <https://doi.org/10.1007/s11269-015-1034-7>
- Garcia-Fresca, B., & Sharp, J. M., Jr. (2005). Hydrogeologic considerations of urban development: Urban-induced recharge. *Geological Society of America Reviews in Engineering Geology*, XVI, 123–126.
- Genereux, D. (1998). Quantifying uncertainty in tracer-based hydrograph separations. *Water Resources Research*, 34(4), 915–919. <https://doi.org/10.1029/98WR00010>
- Gleick, P. H. (2010). Roadmap for sustainable water resources in southwestern North America. *Proceedings of the National Academy of Sciences*, 107(50), 21300–21305. <https://doi.org/10.1073/pnas.1005473107>
- Global Network of Isotopes in Precipitation & International Atomic Energy Agency. (2014). *IAEA/GNIP Precipitation Sampling Guide*. Retrieved from http://www.naweb.iaea.org/naweb/ih/documents/other/gnip_manual_v2.02_en_hq.pdf
- Gober, P., Quay, R., & Larson, K. L. (2016). Outdoor water use as an adaptation problem: Insights from North American Cities. *Water Resources Management*, 30(3), 899–912. <https://doi.org/10.1007/s11269-015-1205-6>
- Gómez-Navarro, C., Pataki, D. E., Bowen, G. J., & Oerter, E. J. (2019). Spatiotemporal variability in water sources of urban soils and trees in the semiarid, irrigated Salt Lake Valley. *Ecohydrology*, 12(8). <https://doi.org/10.1002/eco.2154>
- Gonzales, P., & Ajami, N. (2017). Social and Structural Patterns of Drought-Related Water Conservation and Rebound. *Water Resources Research*, 53, 10619–10634. <https://doi.org/10.1002/2017WR021852>
- Grimmond, C. S. B., & Oke, T. R. (1986). Urban water balance: 2. Results from a Suburb of Vancouver, British Columbia. *Water Resources Research*, 22, 1404–1412. <https://doi.org/10.1029/WR022i010p01404>
- Harvey, F. E. (2005). Stable hydrogen and oxygen isotope composition of precipitation in Northeastern Colorado. *Journal of the American Water Resources Association*, 41(2), 447–460. <https://doi.org/10.1111/j.1752-1688.2005.tb03748.x>
- Hibbs, B. J., Hu, W., & Ridgway, R. (2012). Origin of stream flows at the wildlands-urban Interface, Santa Monica Mountains, California, U.S.A. *Environmental and Engineering Geoscience*, 18(1), 51–64. <https://doi.org/10.2113/gsegeosci.18.1.51>
- Hopkins, K. G., Morse, N. B., Bain, D. J., Bettez, N. D., Grimm, N. B., Morse, J. L., et al. (2015). Assessment of regional variation in stream-flow responses to urbanization and the persistence of physiography. *Environmental Science & Technology*, 49(5), 2724–2732. <https://doi.org/10.1021/es505389y>
- International Atomic Energy Agency. (2015). *WISER – Water isotope system for data analysis, visualization and electronic retrieval*. Retrieved from <https://nucleus.iaea.org/>
- Jameel, Y., Brewer, S., Fiorella, R. P., Tipple, B. J., Terry, S., & Bowen, G. J. (2018). Isotopic reconnaissance of urban water supply system dynamics. *Hydrology and Earth System Sciences*, 22(11), 6109–6125. <https://doi.org/10.5194/hess-22-6109-2018>
- Jameel, Y., Brewer, S., Good, S. P., Tipple, B. J., Ehleringer, J. R., & Bowen, G. J. (2016). Tap water isotope ratios reflect urban water system structure and dynamics across a semiarid metropolitan area: Water Isotope Reflects Urban Water Dynamics. *Water Resources Research*, 52(8), 5891–5910. <https://doi.org/10.1002/2016WR019104>
- Jefferson, A. J., Bell, C. D., Clinton, S. M., & McMillan, S. K. (2015). Application of isotope hydrograph separation to understand contributions of stormwater control measures to urban headwater streams: Isotope hydrograph separation to characterize urban stormwater dynamics. *Hydrological Processes*, 29(25), 5290–5306. <https://doi.org/10.1002/hyp.10680>
- Kampf, S. K., Burges, S. J., Hammond, J. C., Bhaskar, A., Covino, T. P., Eurich, A., et al. (2020). The case for an open water balance: Reenvisioning network design and data analysis for a complex, uncertain world. *Water Resources Research*, 56. <https://doi.org/10.1029/2019WR026699>
- Karamouz, M., Moridi, A., & Nazif, S. (2010). *Urban water engineering and management*. CRC Press.
- Kaushal, S. S., & Belt, K. T. (2012). The urban watershed continuum: Evolving spatial and temporal dimensions. *Urban Ecosystems*, 15(2), 409–435. <https://doi.org/10.1007/s11252-012-0226-7>
- Kendall, C., & McDonnell, J. J. (1999). *Isotope Tracers in Catchment Hydrology (developments in Water Science)*. Elsevier Science.
- Kuhlemann, L.-M., Tetzlaff, D., Smith, A., Kleinschmit, B., & Soulsby, C. (2021). Using soil water isotopes to infer the influence of contrasting urban green space on ecohydrological partitioning. *Hydrology and Earth System Sciences*, 25(2), 927–943. <https://doi.org/10.5194/hess-25-927-2021>
- Kuhlemann, L.-M., Tetzlaff, D., & Soulsby, C. (2020). Urban water systems under climate stress: An isotopic perspective from Berlin, Germany. *Hydrological Processes*, 34(18), 3758–3776. <https://doi.org/10.1002/hyp.13850>
- Leonard Rice Engineers, Inc. (2015). *Colorado water entities*. Retrieved from <http://www.lre-projects.com/ColoradoWaterEntities/>
- Lerner, D. N. (2002). Identifying and quantifying urban recharge: A review. *Hydrogeology Journal*, 10(1), 143–152. <https://doi.org/10.1007/s10040-001-0177-1>

- Litvak, E., Manago, K. F., Hogue, T. S., & Pataki, D. E. (2017). Evapotranspiration of urban landscapes in Los Angeles, California at the municipal scale: Evapotranspiration of urban landscapes. *Water Resources Research*, 53(5), 4236–4252. <https://doi.org/10.1002/2016WR020254>
- Manago, K. F., & Hogue, T. S. (2017). Urban streamflow response to imported water and water conservation policies in Los Angeles, California. *Journal of the American Water Resources Association*, 626–640. <https://doi.org/10.1111/1752-1688.12515>
- McPherson, T. N., Burian, S. J., Stenstrom, M. K., Turin, H. J., Brown, M. J., & Suffet, I. H. (2005). Dry and wet weather flow nutrient loads from a Los Angeles Watershed. *JAWRA Journal of the American Water Resources Association*, 41(4), 959–969. <https://doi.org/10.1111/j.1752-1688.2005.tb03780.x>
- Musgrove, M., Beck, J. A., Paschke, S. S., Bauch, N. J., & Mashburn, S. L. (2014). *Quality of Groundwater in the Denver Basin Aquifer System, Colorado, 2003-5* (No. U.S. Geological Survey Scientific Investigations Report 2014–5051). US Geological Survey. <https://doi.org/10.3133/sir20145051>
- NOAA. (2020). *Climate normals at DENVER/STAPLETON INT'L AP CO 1961-1990*. June 9, 2020. Retrieved from ftp://ftp.atdd.noaa.gov/pub/GCOS/WMO-Normals/TABLES/REG_IV/US/GROUP3/72469.TXT
- Oad, R., & DiSpigno, M. (1997). Water rights to return flow from urban landscape irrigation. *Journal of Irrigation and Drainage Engineering*, 123(4), 293–299. [https://doi.org/10.1061/\(asce\)0733-9437\(1997\)123:4\(293\)](https://doi.org/10.1061/(asce)0733-9437(1997)123:4(293))
- Oerter, E. J., & Bowen, G. (2017). In situ monitoring of H and O stable isotopes in soil water reveals ecohydrologic dynamics in managed soil systems. *Ecohydrology*, 10(4), e1841. <https://doi.org/10.1002/eco.1841>
- Palmex, Ltd. (2019). *Palmex rain sampler RS1*. Retrieved from <http://www.rainsampler.com/portfolio-page/rain-sampler-rs1/>
- Passarello, M. C., Sharp, J. M., & Pierce, S. A. (2012). Estimating urban-induced artificial recharge: A Case Study for Austin, TX. *Environmental & Engineering Geoscience*, 18(1), 25–36. <https://doi.org/10.2113/gsegeosci.18.1.25>
- Quesnel, K. J., & Ajami, N. K. (2017). Changes in water consumption linked to heavy news media coverage of extreme climatic events. *Science Advances*, 3(10), e1700784. <https://doi.org/10.1126/sciadv.1700784>
- R Core Team. (2019). *R: A Language and Environment for Statistical Computing*. Vienna, Austria. R Foundation for Statistical Computing. Retrieved from <https://www.R-project.org/>
- Reich, P., McMaster, D., Bond, N., Metzeling, L., & Lake, P. S. (2010). Examining the ecological consequences of restoring flow intermittency to artificially perennial lowland streams: Patterns and predictions from the Broken—Boosey creek system in northern Victoria, Australia. *River Research and Applications*, 26(5), 529–545. <https://doi.org/10.1002/rra.1265>
- Riley, S. P. D., Busteed, G. T., Kats, L. B., Vandergon, T. L., Lee, L. F. S., Dagit, R. G., et al. (2005). Effects of urbanization on the distribution and abundance of amphibians and invasive species in Southern California streams. *Conservation Biology*, 19(6), 1894–1907. <https://doi.org/10.1111/j.1523-1739.2005.00295.x>
- Rolls, R. J., Leigh, C., & Sheldon, F. (2012). Mechanistic effects of low-flow hydrology on riverine ecosystems: Ecological principles and consequences of alteration. *Freshwater Science*, 31(4), 1163–1186. <https://doi.org/10.1899/12-002.1>
- RStudio Team. (2020). *RStudio: Integrated Development Environment for R Boston, MA: RStudio*. PBC. Retrieved from <http://www.rstudio.com/>
- Sabo, J. L., Sinha, T., Bowling, L. C., Schoups, G. H. W., Wallender, W. W., Campana, M. E., et al. (2010). Reclaiming freshwater sustainability in the Cadillac Desert. *Proceedings of the National Academy of Sciences*, 107(50), 21263–21269. <https://doi.org/10.1073/pnas.1009734108>
- Sanzana, P., Gironás, J., Braud, I., Muñoz, J.-F., Vicuña, S., Reyes-Paecke, S., et al. (2019). Impact of urban growth and high residential irrigation on streamflow and groundwater levels in a peri-urban semiarid catchment. *Journal of the American Water Resources Association*, 0(0). <https://doi.org/10.1111/1752-1688.12743>
- Shah, J. J. F., Jameel, Y., Smith, R. M., Gabor, R. S., Brooks, P. D., & Weintraub, S. R. (2019). Spatiotemporal variability in water sources controls chemical and physical properties of a semi-arid urban river system. *Journal of the American Water Resources Association*, 55(3), 591–607. <https://doi.org/10.1111/1752-1688.12734>
- Soulsby, C., Birkel, C., & Tetzlaff, D. (2014). Assessing urbanization impacts on catchment transit times. *Geophysical Research Letters*, 41, 442–448. <https://doi.org/10.1002/2013GL058716>
- Stein, E. D., & Ackerman, D. (2007). Dry weather water quality loadings in arid, urban watersheds of the Los Angeles Basin, California, USA. *JAWRA Journal of the American Water Resources Association*, 43(2), 398–413. <https://doi.org/10.1111/j.1752-1688.2007.00031.x>
- Strange, E. M., Fausch, K. D., & Covich, A. P. (1999). Sustaining ecosystem services in human-dominated watersheds: Biohydrology and ecosystem processes in the South Platte River Basin. *Environmental Management*, 24(1), 39–54. <https://doi.org/10.1007/s002679900213>
- Toor, G. S., Occhipinti, M. L., Yang, Y.-Y., Majcherek, T., Haver, D., & Oki, L. (2017). Managing urban runoff in residential neighborhoods: Nitrogen and phosphorus in lawn irrigation driven runoff. *Plos One*, 12(6), e0179151. <https://doi.org/10.1371/journal.pone.0179151>
- Townsend-Small, A., Pataki, D. E., Liu, H., Li, Z., Wu, Q., & Thomas, B. (2013). Increasing summer river discharge in southern California, USA linked to urbanization. *Geophysical Research Letters*, 40, 4643–4647. <https://doi.org/10.1002/grl.50921>
- USDA. (2018). *Natural Resources Conservation Service: Geospatial data gateway*. August 20, 2020. Retrieved from <https://datagateway.nrcs.usda.gov/>
- USGS. (2020). *StreamStats: Streamflow statistics and spatial analysis tools for water-resources applications*. Retrieved from <https://www.streamstats.usgs.gov/ss/>
- Wallace, S., Biggs, T., Lai, C.-T., & McMillan, H. (2021). Tracing sources of stormflow and groundwater recharge in an urban, semi-arid watershed using stable isotopes. *Journal of Hydrology: Regional Studies*, 34, 100806. <https://doi.org/10.1016/j.ejrh.2021.100806>
- Wang, S., Zhang, M., Che, Y., Zhu, X., & Liu, X. (2016). Influence of below-cloud evaporation on deuterium excess in precipitation of arid Central Asia and its meteorological controls. *Journal of Hydrometeorology*, 17(7), 1973–1984. <https://doi.org/10.1175/JHM-D-15-0203.1>
- Waterisotopes Database. (2019). *Query: Country = US, State/Province = CO, Type = Tap, Project ID = 00099 and 00225, Contact Name = Gabriel Bowen, Project Name = 2019 Groundwater*. Accessed 2019. Retrieved from <http://waterisotopesDB.org>
- Welker, J. M. (2000). Isotopic ($\delta^{18}\text{O}$) characteristics of weekly precipitation collected across the USA: An initial analysis with application to water source studies. *Hydrological Processes*, 14(8), 1449–1464. [https://doi.org/10.1002/1099-1085\(20000615\)14:8<1449::AID-HYP993>3.0.CO;2-7](https://doi.org/10.1002/1099-1085(20000615)14:8<1449::AID-HYP993>3.0.CO;2-7)